Iranian Journal of Chemical Engineering
Vol. 13, No. 4 (Autumn 2016), IAChE

An Investigation of Heat and Mass Transfer Enhancement of Air Dehumidification with Addition of γ-Al_2O_3 Nano-Particles to Liquid Desiccant

L. Omidvar Langroudi[1], H. Pahlavanzadeh[2*], S. Nanvakenari[2]

[1]*Department of Chemistry, Islamic Azad University, Chalus Branch, P.O. Box 46615-397, Iran*
[2]*Faculty of Chemical Engineering, Tarbiat Modares University, Tehran, P.O. Box 14155-143, Iran*

ARTICLE INFO

Article history:
Received: 2015-11-08
Accepted: 2016-02-03

Keywords:
Liquid Desiccant
Dehumidification
RSM
Nano-Particles
Mass Transfer
Heat Transfer

ABSTRACT

The current research aims at conducting an experimental and theoretical investigation on the performance of air dehumidification system using a nanofluid of γ-alumina nano-particles in LiBr/H_2O, as a desiccant. Comparative experiments organized using a central composite design are carried out to evaluate the effects of six numerical indices (air velocity, desiccant flow rate, air humidity ratio, desiccant solution concentration, air temperature, desiccant temperature) and one categorical factor (adding nano-particles), on outlet air humidity ratio and outlet air temperature as responses. Reduced quadratic regression models are derived for each response. The obtained results revealed that LiBr/H_2O solution concentration and air temperature have the most significant effect on outlet air humidity ratio and outlet air temperature, respectively. It was found that the average rates of mass transfer and heat transfer increased to 12.23 % and 13.22 %, respectively, when γ-alumina nano-particles (0.02 wt %) were added to the LiBr/H_2O solution. The average rates of mass and heat transfer coefficients increased to 22.73 % and 26.51 %, respectively.

1. Introduction

It is often essential to control and decrease moisture content of air in hot and humid areas. Although there are many ways to accomplish this, a liquid desiccant system is most attractive because of its flexibility of operation and ability to remove airborne pollutants at a lower regeneration temperature such as that produced by solar energy. In liquid desiccant systems, the moisture of air is removed by bringing it into contact with a liquid desiccant such as TEG, LiBr, LiCl or $CaCl_2$ solution sprinkled on the dehumidification unit. The weak desiccant is concentrated as it heats in

*Corresponding author: pahlavzh@modares.ac.ir

the regeneration unit. The difference between the liquid desiccant and the air, in surface vapor pressure, is driving force for mass transfer [1-2]. Researchers have intensively studied liquid desiccant systems. Several studies have used hygroscopic salts to analyze the physical properties of liquid desiccant and develop new materials [3-4]. Performance evaluations using numerical analysis and/or experimental methods have been introduced [5-8]. Three main models for the analysis of dehumidification are the finite difference model, the effectiveness *NTU* model, and the model based on fitted algebraic equations [9-13]. A number of air handling systems using liquid desiccant and technological improvements and optimization have been proposed [14-16].

The present study examined the effect of adding γ-alumina nano-particles to $LiBr/H_2O$ solution as a desiccant for dehumidification. Recent studies have focused on increasing heat and mass transfer rates using nanofluids. A nanofluid is a fluid in which nano-particles of less than 100 nm in diameter are stably suspended in a base fluid [17-19]. Many researchers examined heat transfer in nanofluids. Most studies considered enhanced heat characteristics of nanofluids, such as convective heat transfer coefficient and thermal conductivity relative to their base fluids [20-22]. Alumina and copper oxide are the most common and inexpensive nanoparticles used in many experimental investigations [17]. Few studies have been conducted to examine enhancement of mass characteristics of nanofluids, such as diffusion coefficient and mass transfer coefficient [23-25].

There are limited researches on heat and mass transfer in nanofluids. Kang et al. [26] studied the vapor absorption and heat transfer rates in falling film flow of nanofluids containing $LiBr/H_2O$ solution with nano-particles of Fe and carbon nanotubes (CNTs). They showed that vapor absorption was higher than for fluids without nano-particles and that mass transfer rate increase was much more significant than heat transfer rate increase in nanofluids, and CNT was better than Fe. Kim et al. [27] measured the vapor absorber performance by SiO_2 nano-particles in $LiBr/H_2O$ nanofluid. They showed that the maximum increase in the heat and mass transfer rates was 46.8 % and 18 %, respectively, when the concentration of SiO_2 nano-particles was 0.005 vol %.

Built upon these findings, the present study was to carry out comparative experiments on air dehumidification using $LiBr/H_2O$ solution with and without γ-alumina nano-particles as a desiccant. The central composite design (CCD) was used to analyze dehumidification using a minimal number of experiments by varying six numerical influential factors (air velocity, desiccant flow rate, air humidity ratio, desiccant solution concentration, air temperature, desiccant temperature) and one categorical factor (adding nano-particles). Mass and heat transfer coefficients were also evaluated and compared.

2. Method

2.1. Preparation of nanofluid

Preparation of a stabilized nanofluid is very important. There are single-step and two-step techniques for producing nanofluids. In the single step technique, nanoparticle production

and nanofluid preparation are done simultaneously; in the two-step technique dry nanoparticles/nanotubes are first produced and then dispersed in a suitable liquid [17,27]. The two-step method was applied in the present study. In experimental testing, γ-alumina nano-particles were used with an average diameter of 10-20 nm and 99.995 % purity (TECNAN, Spain). The nano-particles, suspended in deionized water, were precisely measured to the required weight using an electronic balance. An ultrasonic disruptor (Hielscher up 400s, 400 W, 24 kHz) statically stabilized the nanofluid, which was then mixed with $LiBr/H_2O$ using a magnetic stirrer. Figure 1 depicts dispersion of nano-particles in the base fluid, both without and with ultrasonic stabilization. As indicated, the stabilized particles are homogenously dispersed throughout the base fluid in an acceptable way.

2.2. Experimental setup

Figure 2 shows a detailed scheme of a counter flow dehumidification system. The air supplied by a fan passes through a heater composed of many elements and then passes through a humidifying system. Water is pumped from a water tank above the humidifier and a valve controls water flow. The rate of processed air was adjusted with a rate-modifying inverter. The processed air was drawn from the bottom into the dehumidification column, which is a fiberglass tube with 50 cm height and 8 cm diameter. Glass beads, 1.73 cm in diameter, with a height of 35 cm, were used as packing and had a specific surface area of 264.56 m^2/m^3. The desiccant was adjusted to desired temperature and concentration, stored in tank

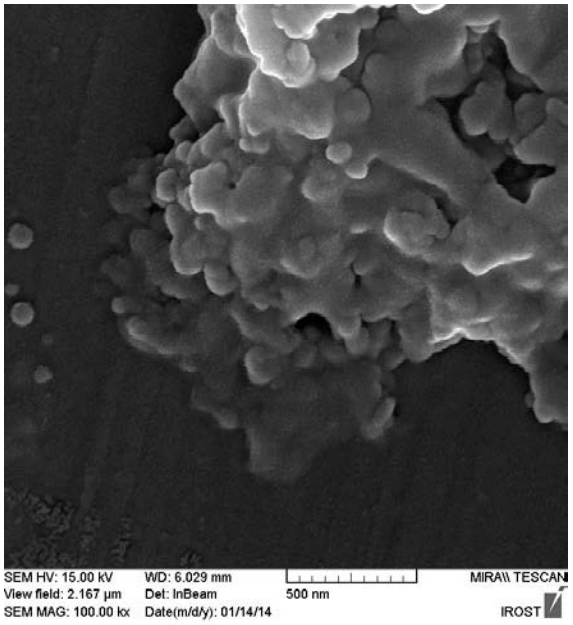

(a)

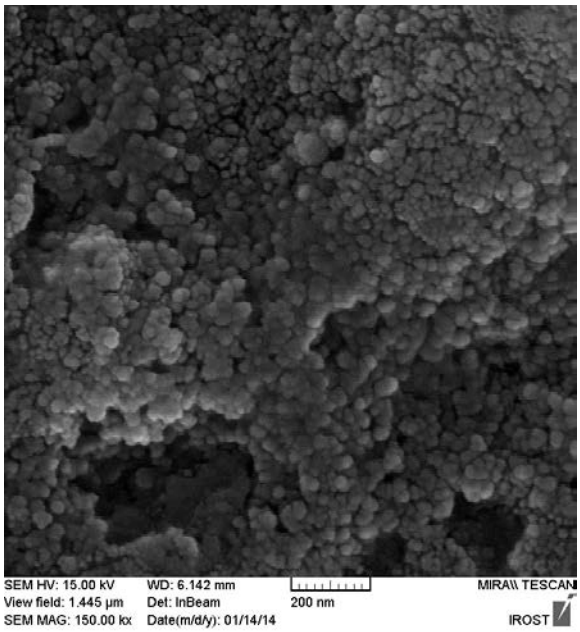

(b)

Figure 1. SEM micrographs of: (a) clotted sample of Al_2O_3 nano-particles in $LiBr/H_2O$ nanofluid without ultrasonic stabilization and (b) dispersed sample of Al_2O_3 nano-particles in $LiBr/H_2O$ nanofluid with ultrasonic stabilization.

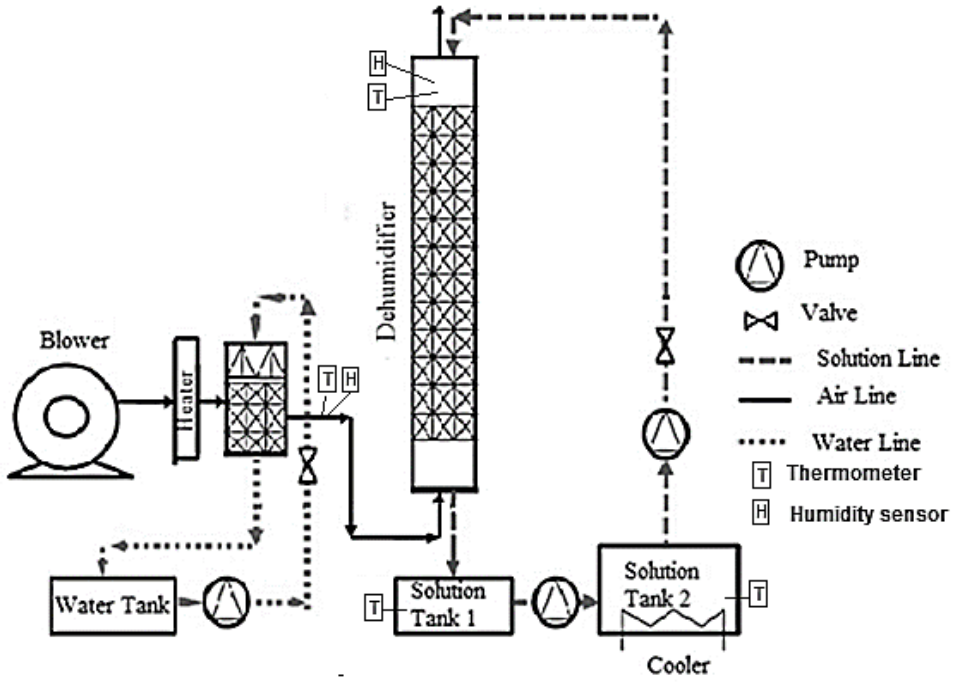

Figure 2. Schematic of the experimental set up.

2 and pumped to the top of the dehumidifier through a flow sensor. After air dehumidification, the desiccant is partially dilute and warm from the released latent heat and collects at the bottom of the dehumidifier (tank 1). The intervening pump transfers the desiccant to tank 2. The temperature is reduced in the cooling coils in tank 2. The temperature and humidity of the air is measured before entering and after leaving the dehumidification column. Table 1 gives the main specifications of the measuring devices used during experimentation.

2.3. Heat and mass transfer model

The liquid desiccant is brought into direct contact with the processed air in the dehumidifier. The moisture transfers from the air to the desiccant because the vapor partial pressure of the air is higher than that on the

Table 1
Measuring devices specifications.

Parameter	Device	Accuracy	Operative range
Air temperature	Pt 100 RTDs	0.1˚C	0-100˚C
Solution temperature	Digital RTD	0.1˚C	0-100˚C
Desiccant density	Hydrometer	1 kg/m^3	1200-1300 kg/m^3
			1300-1400 kg/m^3
			1400-1500 kg/m^3
Desiccant flow rate	Rotameter	0.25 L/min	0.75-7.5 L/min
Air rate	Anemometer	2 %	0-20 m/s
Air relative humidity	Testo 445	1 %	0-100 %

surface of the desiccant solution. The liquid desiccant temperature increases as heat of absorption. This means that mass transfer and heat transfer are coupled. The basic steady state mass and energy balance equations, based on the effectiveness of *NTU* model for a typical control volume (Figure 3) are [5,10]:

$$\frac{d\omega_a}{dV} = \frac{NTU}{V}\left(\omega_{Ts,sat} - \omega_a\right) \quad (1)$$

$$\frac{dh_a}{dV} = \frac{NTU.Le}{V}\left[\left(h_{Ts,sat} - h_a\right) + \lambda.\left(\frac{1}{Le} - 1\right)\left(\omega_{Ts,sat} - \omega_a\right)\right] \quad (2)$$

Where, ω_a is the air humidity ratio, V is the total volume of the dehumidifier, $h_{Ts,sat}$ and $\omega_{Ts,sat}$ are the air enthalpy and humidity ratio in equilibrium with the desiccant, respectively, and λ is the latent heat of vaporization.

The Lewis number and *NTU* are defined as:

$$Le = \frac{h_c}{h_D C_{pa}} \quad (3)$$

$$NTU = \frac{h_D a_w V}{G_a} \quad (4)$$

Where, h_C and h_D are the heat and mass transfer coefficients, respectively, C_{pa} is the specific heat capacity of the humid air, a_w is the wetted surface area of the packing, and G_a is the mass flow rate of the air. The method used to solve the effectiveness model has been described by Pahlavanzadeh and Nooriasl [5]. The h_D-*Le* separative evaluation method [28] was applied to determine the coupled mass and heat transfer coefficients.

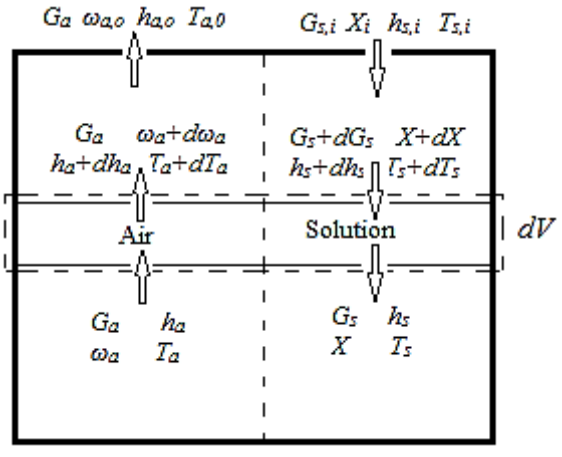

Figure 3. Sketch of countercurrent dehumidification.

2.4. Experimental design and data analysis

Response surface methodology (RSM) is an effective statistical tool for regression modeling and analysis of multiple factor processes. The popular regression model, CCD under RSM, was used to design the dehumidification experiments to determine the relevant information and the relationship between factors affecting the output responses without a large number of design points [13,20-30]. The effects of six numerical factors (air velocity, A; desiccant flow rate, B; air humidity ratio, C; desiccant solution concentration, D; air temperature, E; and desiccant temperature, F) at five levels and one categorical factor (adding nano-particles, G) were considered (Table 2). The output responses were outlet air humidity ratio and outlet air temperature. The experimental design matrix consisted of 172 run experiments; the output responses are shown in Appendix A. The concentration of nano-particles was constant (0.02 wt %) in all experiments using nano-particles. The response function (y) is widely related to factors x_i and x_j by the following second order polynomial equation:

$$y = b_0 + \sum b_i x_i + \sum b_{ii} x_i^2 + \sum b_{ij} x_i x_j \quad (5)$$

Table 2
The experimental range and levels of the independent factors in the CCD.

Variable	Low axial (-α)	Low factorial (-1)	Center	High factorial(+1)	High axial(+α)
x_1(A): Air velocity (m/s)	2.5	2.9	3.5	4.1	4.5
x_2(B): Desiccant flow rate (kg/s)	0.012	0.017	0.026	0.035	0.04
x_3(C): Air humidity ratio (kg/kg)	0.0118	0.0133	0.0159	0.0185	0.0200
x_4(D): Desiccant concentration (kg/kg)	0.38	0.040	0.44	0.48	0.50
x_5(E): Air temperature (˚C)	25	27.7	32.5	37.3	40
x_6(F): Desiccant temperature (˚C)	20	21.8	25	28.2	30
x_7(G): adding nano-particles (0.02 wt %)	-	no	-	yes	-

Where, b_0 is a constant, b_i is a linear coefficient, b_{ii} is a square coefficient, and b_{ij} is an interaction coefficient [31]. The experimental data was analyzed using a commercial statistical software, Design-Expert version 7.

3. Results and discussion

3.1. Regression model and statistical analysis

All data were statistically analyzed to determine the significant main effects and the interaction effects of factors. Analysis of variance (ANOVA) results for the quadratic regression models of all responses are shown in Table 3. As it can be seen, the quadratic regressions for outlet air humidity ratio and outlet air temperature are significant at a 95 % confidence interval (p value < 0.0001). At values less than 0.05 for Prob > F (p values), the regression terms are significant. A larger F value and smaller p value will increase the significance of the corresponding coefficient [32]. The levels of significance of all factors and interactions are shown in Table 3.

It is evident that, of the linear terms and quadratic terms, D ($X_{s,i}$) and DF ($X_{s,i}$ $T_{s,i}$) have the greatest effects on outlet air humidity ratio and E ($T_{a,i}$) and EF ($T_{a,i}$ $T_{s,i}$) have the most influence on outlet air temperature. The use of manual regression eliminated the insignificant interaction terms and allowed the reduced quadratic regression models to be derived. ANOVA test results are summarized in Table 4. As indicated, the reduced quadratic regression models were significant at p value < 0.0001 for each response. The relatively high values of the predicted and adjusted R^2 (close to 1) are desirable and ensure that the reduced quadratic regression models are capable of representing the system under the given experimental domain [33]. A value of >0.98 indicates that the mathematical regression could explain most of the variability in each response. The range of the predicted values in the design are measured precisely, ensuring an average prediction error ratio [34]. Ratios of >4 support the fitness of the regression model and were

Table 3
ANOVA for the response surface quadratic models.

Source	df	Outlet air humidity ratio ($\omega_{a,o}$)				Outlet air temperature ($T_{a,o}$)			
		Sum of squares	F value	p-value	Remark	Sum of squares	F value	p-value	Remark
Model	34	5.876E-004	332.97	<0.0001	a	1063.77	409.35	<0.0001	a
A-$U_{a,i}$	1	5.225E-006	100.68	<0.0001	a	17.95	234.90	<0.0001	a
B- $G_{s,i}$	1	6.821E-006	131.42	<0.0001	a	0.40	5.25	0.0235	b
C-$\omega_{a,i}$	1	1.716E-004	3306.87	<0.0001	a	3.208E-003	0.042	0.8380	c
D- $X_{s,i}$	1	1.949E-004	3755.14	<0.0001	a	44.90	587.50	<0.0001	a
E- $T_{a,i}$	1	2.125E-006	40.95	<0.0001	a	550.14	7197.81	<0.0001	a
F- $T_{s,i}$	1	9.003E-005	1734.74	<0.0001	a	321.11	4201.26	<0.0001	a
G-nanoparticles	1	5.683E-006	109.50	<0.0001	a	15.01	196.38	<0.0001	a
AB	1	0	0	1	c	0.018	0.23	0.6323	c
AC	1	5.181E-007	9.98	0.0019	b	0.040	0.52	0.4733	c
AD	1	6.518E-007	12.56	0.0005	b	0.87	11.42	0.0009	b
AE	1	3.781E-008	0.73	0.3948	c	2.62	34.23	<0.0001	a
AF	1	2.785E-007	5.73	0.0220	b	1.30	17.00	<0.0001	a
AG	1	1.514E-006	0.9	0.3457	c	9.632E-003	0.13	0.7231	c
BC	1	1.387E-006	29.16	<0.0001	a	0.0190	0.24	0.6223	c
BD	1	3.781E-008	26.73	<0.0001	a	0.010	0.13	0.7142	c
BE	1	8.712E-007	0.73	0.3948	c	0.86	11.27	0.0010	b
BF	1	6.456E-008	16.79	<0.0001	a	8.290E-003	0.11	0.7424	c
BG	1	6.456E-008	1.24	0.2667	c	0.032	0.42	0.5187	c
CD	1	1.784E-010	3.438E-003	0.9533	c	1.86	24.31	<0.0001	a
CE	1	6.618E-009	0.13	0.7216	c	0.73	9.58	0.0024	b
CF	1	5.397E-007	10.40	0.0016	b	1.67	21.81	<0.0001	a
CG	1	1.409E-006	27.15	<0.0001	a	0.060	0.79	0.3753	c
DE	1	4.159E-008	0.80	0.3722	c	0.13	1.75	0.1887	c
DF	1	3.911E-006	75.36	<0.0001	a	0.061	0.79	0.3743	c
DG	1	6.395E-007	12.32	0.0006	b	0.10	1.32	0.2535	c
EF	1	6.898E-009	0.13	0.7160	c	7.56	98.94	<0.0001	a
EG	1	2.195E-008	0.42	0.5166	c	6.74	88.17	<0.0001	a
FG	1	4.887E-007	9.42	0.0026	b	4.01	52.43	<0.0001	a
A^2	1	4.207E-008	0.81	0.3695	c	0.030	0.39	0.5353	c
B^2	1	2.806E-007	5.41	0.0215	b	0.14	1.78	0.1840	c
C^2	1	1.273E-010	2.453E-003	0.9606	c	0.18	2.34	0.1281	c
D^2	1	1.265E-006	24.37	<0.0001	a	0.30	3.97	0.0484	b
E^2	1	3.013E-008	0.58	0.4474	c	0.043	0.56	0.4556	c
F^2	1	1.135E-006	21.86	<0.0001	a	0.31	4.05	0.0462	b
Residual	137	7.110E-006				10.47			
Lack of Fit	119	6.957E-006	6.88	<0.0001	a	10.29	8.65	<0.0001	a
Pure Error	18	1.530E-007				0.18			
Cor Total	171	5.947E-004				1074.24			

a: highly significant, b: significant, c: not significant

Table 4
Statistical results of the ANOVA for the reduced quadratic model.

Response	Correlation in terms of actual significant factors	P-value	R^2	Adj.R^2	Adequate Precision	CV %
$\omega_{a,o}$		<0.0001	0.989	0.986	82.204	1.74
(I)	0.041349 - 0.0014604A + 0.057519B + 0.24866C - 0.15306D + 0.0000356716E +0.0001826668F + 0.0459AC + 0.00295762AD - 0.0000102094AF - 4.0027BC - 0.37644BD +0.00366053BF + 0.00839842CF - 0.00169092DF +1.05969 B^2+ 0.18544D^2 + 0.0000128147F^2					
(II)	0.042352 - 0.0014604A + 0.057519B + 0.174C - 0.15607D + 0.0000356716E +0.000225705F + 0.0459AC + 0.00295762AD -0.0000102094AF-4.0027BC-0.37644BD +0.00366053BF+0.00839842CF-0.00169092DF +1.05969 B^2+ 0.18544D^2 + 0.0000128147F^2					
$T_{a,o}$		<0.0001	0.989	0.987	85.230	1.03
(I)	-10.28088 - 1.69194A + 32.74126B + 831.54964C - 4.61884D + 0.68133E + 0.96641F + 3.63474AD + 0.057302 AE - 0.048597AF - 1.17359BE - 1132.77161CD + 2.289CE – 15.91108CF - 0.016857EF – 7.37208D^2 + 0.010435F^2					
(II)	-11.36681 - 1.69194A + 32.74126B + 831.54964C - 4.61884D + 0.59492E + 1.09539F + 3.63474AD + 0.057302 AE - 0.048597AF - 1.17359BE - 1132.77161CD + 2.289CE – 15.91108CF - 0.016857EF – 7.37208D^2 + 0.010435F^2					

(I): without the addition nano-particles to LiBr/H_2O desiccant, (II): with the addition nano-particles to LiBr/H_2O desiccant

82.204 and 85.230 for outlet air humidity ratio and outlet air temperature regression models, respectively. Low values of the coefficient of variation (CV; <10) indicate good accuracy and reliability of the experiments [13]. Diagnostic plots of the predicted versus actual values for each response are shown in Fig. 4. It indicates satisfactory correlation between the experimental data and the mathematical model predictions.

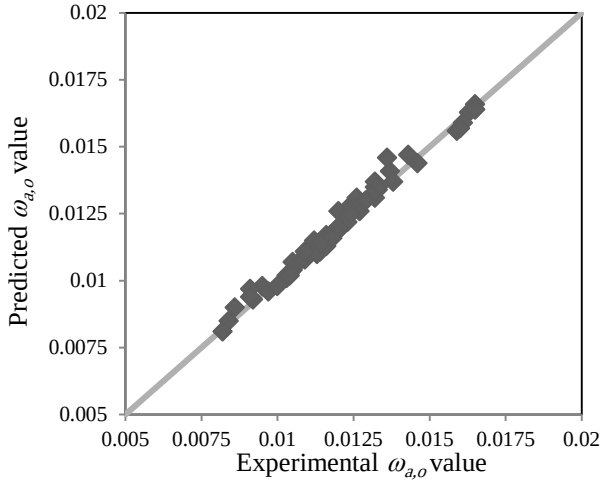

(a)

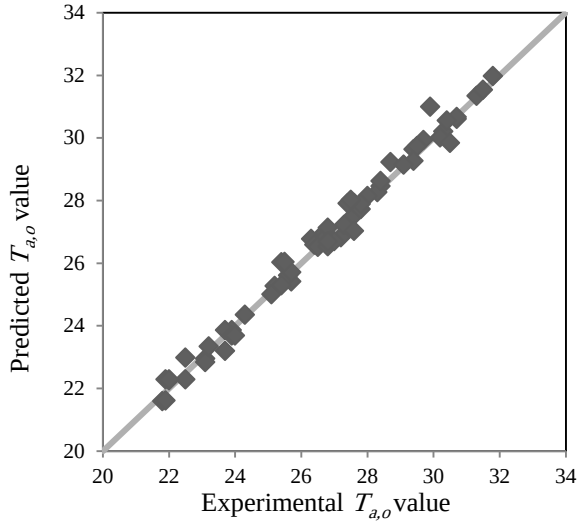

(b)

Figure 4. Actual and predicted plots of: (a) outlet air humidity ratio (b) outlet air temperature.

3.2. Response surface plots

The 3D response surfaces are 3D graphic representations of the reduced quadratic regression models. These were generated for the responses of outlet air humidity ratio and outlet air temperature. Since the regression models have six numerical factors and one categorical factor, several plots were created. Figures 5-8 depict plots of the two factors with large interaction effects on the responses, as indicated by high F values. The two numerical factors were varied while the other factors were kept constant at center values and the categorical factor was studied for a high level (yes).

Figure 5 shows the surface plot of the effects for inlet desiccant concentration and temperature on outlet air humidity ratio. Increasing the desiccant concentration by 31.5 % (0.38 kg/kg to 0.50 kg/kg) decreased outlet air humidity ratio by 25.7 % at a low desiccant temperature and by 31.5 % at a high desiccant temperature. Decreasing the desiccant temperature by 33.3 % (30°C to 20°C) decreased outlet air humidity ratio 25.3 % at low, and 19 % at high desiccant concentrations. This occurred because the desiccant vapor pressure decreased and created a higher potential for mass transfer. These results agree with the observations reported by Moon et al. [6]. Figure 6 illustrates outlet air humidity ratio as a function of inlet air humidity ratio and desiccant flow rate. Decreasing the inlet air humidity ratio by 41 % (0.0200 kg/kg to 0.0118 kg/kg) decreased outlet air humidity ratio by 28.3 % at a low desiccant flow rate and 22.7 % at a high desiccant flow rate. Decreasing the inlet air humidity ratio decreased humidity available for dehumidification. Increasing the desiccant flow rate by 233.3 % (0.012 kg/s to 0.04 kg/s) slightly decreased the outlet air humidity ratio by 1.5 % at low and 8.4 % at high inlet air humidity. The desiccant flow rate was sufficient to ensure wetting of the packing but not cause high variation in the outlet air humidity ratio, as described by Fumo and Goswami [1]. Figure 7 shows the effect of

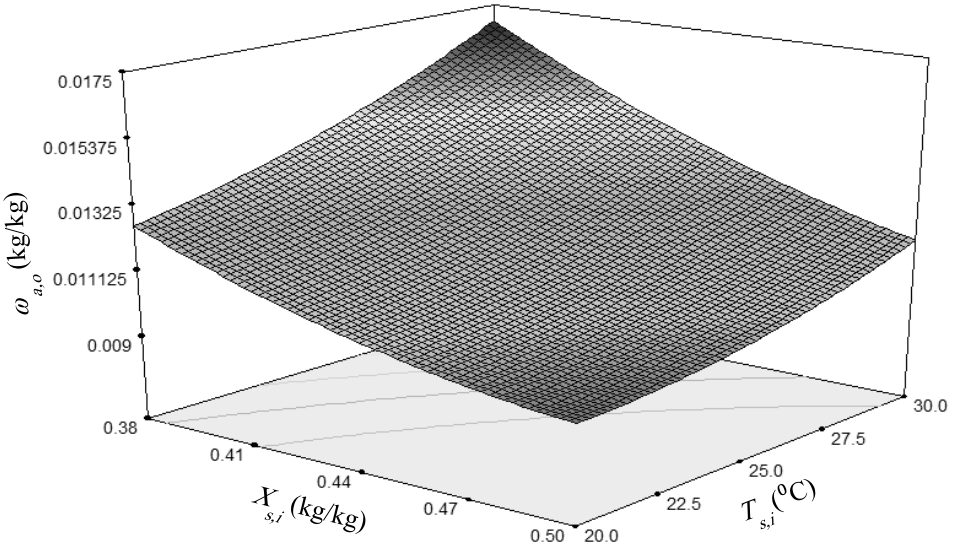

Figure 5. The effect of inlet desiccant cocentration and desiccant temperature on outlet air humidity ratio at $U_{a,i}$=3.5 m/s, $G_{s,i}$=0.026 kg/s, $\omega_{a,i}$=0.0159 kg/kg , $T_{a,i}$=32.5˚C and nanoparticles concentration =0.02 wt %.

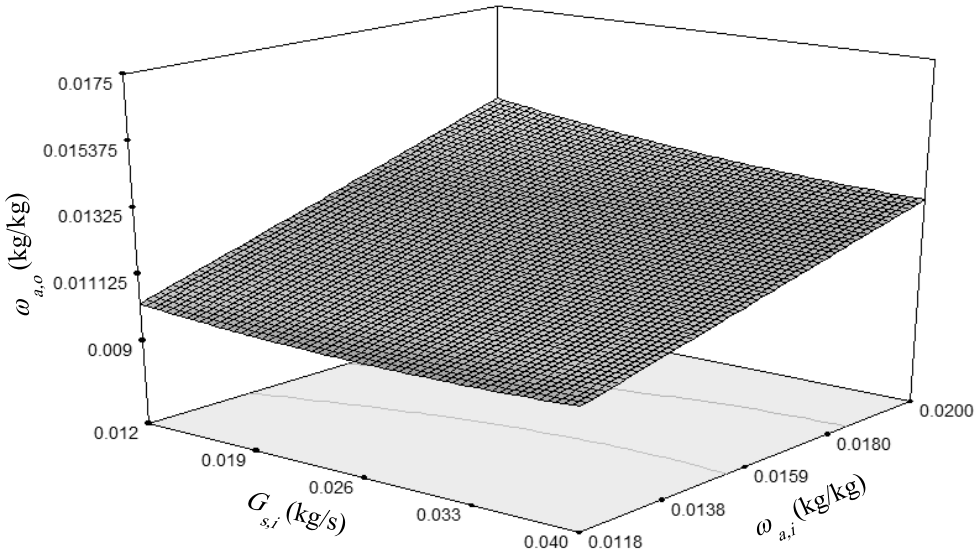

Figure 6. The effect of inlet desiccant flowrate and air humidity ratio on outlet air humidity ratio at $U_{a,i}$=3.5 m/s, $X_{s,i}$=0.44 kg/kg, $T_{s,i}$=25˚C, $T_{a,i}$=32.5˚C and nanoparticles concentration = 0.02 wt %.

inlet air temperature and desiccant temperature on outlet air temperature. Decreasing the inlet air temperature by 37.5 % decreased the outlet air temperature by 25 % at low desiccant temperature and by 13.4 % at high desiccant temperature. Decreasing desiccant temperature by 33.3 % (30°C to 20°C) decreased outlet air temperature by 26.9 % to 15.6 % as the inlet air temperature increased from 25°C to 40°C. The data

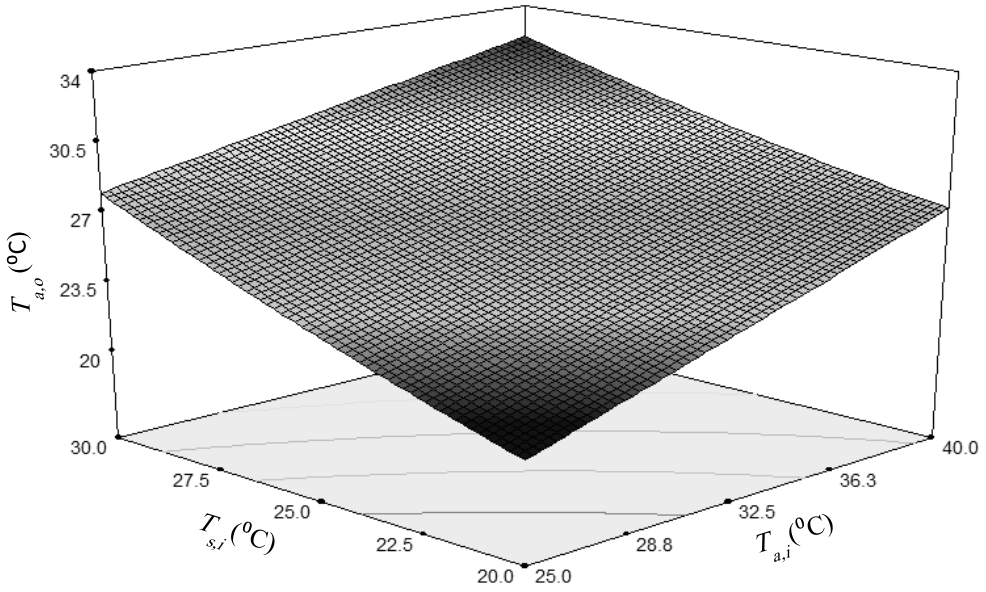

Figure 7. The effect of inlet desiccant temperature and air temperature on outlet air temperature at $U_{a,i}$=3.5 m/s, $X_{s,i}$=0.44 kg/kg, $G_{s,i}$=0.026 kg/s, $\omega_{a,i}$=0.0159 kg/kg and nanoparticles concentration = 0.02 wt %.

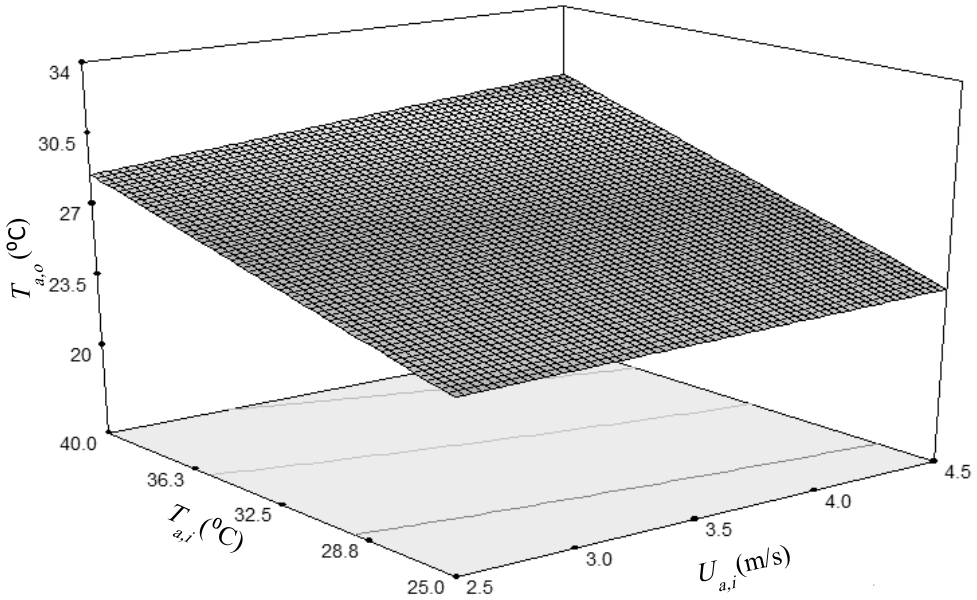

Fig. 8. The effect of inlet air velocity and air temperature on outlet air temperature at $X_{s,i}$=0.44 kg/kg, $G_{s,i}$=0.026 kg/s, $\omega_{a,i}$=0.0159 kg/kg, $T_{s,i}$=25°C and nanoparticles concentration = 0.02 wt %.

showed that outlet air temperature was lower than inlet air temperature; this occurred because the air is cooled through contact with the cooled desiccant. Decreasing the inlet air temperature and desiccant temperature decreased the outlet air temperature. Figure 8

shows the effect of inlet air velocity and temperature on outlet air temperature. Decreasing the air velocity 44.4 % (4.5 m/s to 2.5 m/s) decreased outlet air temperature 1.9 % at low inlet air temperature and 6 % at high inlet air temperature. Decreasing the air velocity increased the residence time between the air and cooled desiccant. The change in air velocity had little effect on outlet air temperature. It is because the specific operating conditions for air velocity allowed sufficient residence time. Decreasing the inlet air temperature, as shown in Fig. 7 decreased the outlet air temperature.

3.3. Statistical optimization

In this study the outlet air humidity and temperature equations (regression models) as objective functions with six numerical variables and one categorical variable are optimized by using Design-Expert software. Two sided inequality constraints are $2.5 \leq U_{a,i} \leq 4.5$, $0.012 \leq G_{s,i} \leq 0.04$, $0.0159 \leq \omega_{a,i} \leq 0.020$, $0.38 \leq X_{s,i} \leq 0.50$, $32.5 \leq T_{a,i} \leq 40$ and $20 \leq T_{s,i} \leq 30$. The result for optimized parameters and validation experiments are presented in Table 5. The optimal values to gain the minimum outlet air humidity and temperature were estimated air velocity 2.7 m/s, desiccant flow rate 0.04 kg/s, air humidity ratio 0.0196 kg/kg, desiccant concentration 0.50 kg/kg, air temperature 32.6 °C, desiccant temperature 20°C and adding nanoparticles. These values gave outlet air humidity and temperature of 0.0093 kg/kg and 21.88 °C, respectively. Additional experiment was carried out to compare between the experimental and predicted outlet air humidity and temperature at optimum condition. The result of the model was in good agreement with the experimental data of 0.0095 kg/kg and 22.2 °C, respectively.

3.4. Effects of γ-alumina nano-particles in LiBr/H_2O solution on responses and mass and heat transfer coefficients

The 172 dehumidification experiments were designed so that two experiments at each level for all six numerical factors are the same as the altered categorical factor. Some experiments (50 runs) were randomly selected to investigate the effect of adding nano-particles. Table 6 lists the changes in air humidity and air temperature, mass and heat transfer rate, and mass and heat transfer coefficients, both with and without the addition of nano-particles to LiBr/H_2O solution. To allow comparison of results,

Table 5
Optimized process conditions with predicted and experimental values of responses.

Parameters	Process conditions (optimized)							Responses (minimized outlet air humidity and temperature)			
	$U_{a,i}$ m/s	$G_{s,i}$ kg/s	$\omega_{a,i}$ kg/kg	$X_{s,i}$ kg/kg	$T_{a,i}$ °C	$T_{s,i}$ °C	Adding nanoparticles	$\omega_{a,o,pre}$ kg/kg	$\omega_{a,o,exp}$ kg/kg	$T_{a,o,pre}$ °C	$T_{a,o,exp}$ °C
value	2.7	0.04	0.0196	0.50	32.6	20	yes	0.0093	0.0095	21.88	22.2

increases in the mass transfer rate (R_G) and heat transfer rate (R_Q) are defined as:

$$R_{Gw} = \left(\frac{(G_w)_{with\ the\ addition\ of\ nanoparticles}}{(G_w)_{without\ the\ addition\ of\ nanoparticles}} - 1\right) \times 100 \quad (6)$$

$$R_Q = \left(\frac{(Q)_{with\ the\ addition\ of\ nanoparticles}}{(Q)_{without\ the\ addition\ of\ nanoparticles}} - 1\right) \times 100 \quad (7)$$

Where, G_w is the mass transfer rate and Q is the heat transfer rate:

$$G_w = G_a \Delta\omega_a = G_a(\omega_{a,i} - \omega_{a,0}) \quad (8)$$

$$Q = G_a C_{pa} \Delta T_a = G_a C_{pa}(T_{a,i} - T_{a,0}) \quad (9)$$

In addition, Table 6 shows the mass and heat transfer coefficients increases (R_{hC} and R_{hD}). As shown, changes in air humidity and air temperature increased when nano-particles were added to the LiBr/H_2O desiccant. Mass transfer rate increased from 4.25 % to 25 % and heat transfer rate increased from 5.26 % to 25 %, with average increases of 12.23 % and 13.22 %, respectively. The addition of nano-particles to LiBr/H_2O desiccant increased the mass transfer coefficient from 19.35 % to 28.12 % and heat transfer coefficient from 20.51 % to 32.35 % with average increases of 22.73 % and 26.51 %, respectively. These increases are considerable. The nano-particles increased heat and mass transfer performance by their convective characteristics of Brownian motion [26-27]. Both the outlet air humidity and temperature decreased after adding the nano-particles, which produced desirable results for the liquid cooling systems.

Table 6

A comparison of mass and heat transfer of LiBr/H_2O solution with and without the addition nano-particles.

Runs with similar conditions of numerical factors	Without the addition nano-particles to LiBr/H_2O desiccant					
	$\Delta\omega_a$ (kg/kg)	ΔT_a (^{0}C)	Gw*10^3 (kg/s)	Q (Kw)	h_D (kg/m^{2}s)	h_C (kW/m^2^{o}C)
1 , 46	0.0038	5.1	0.0752	0.1045	0.036	0.041
3 , 13	0.0048	3.6	0.0796	0.0615	0.035	0.036
20 , 140	0.0009	7.8	0.0144	0.1286	0.032	0.034
12 , 159	0.0040	5.1	0.0792	0.1045	0.039	0.044
38 , 161	0.0076	5.8	0.1262	0.1000	0.032	0.039
56 , 69	0.0042	6.6	0.0949	0.1551	0.034	0.042
84 , 119	0.0018	4.2	0.0301	0.0722	0.034	0.037
98 , 108	0.0020	5.8	0.0320	0.0965	0.032	0.034
64 , 160	0.0049	7.4	0.0970	0.1516	0.037	0.038
88 , 92	0.0042	8.3	0.0672	0.1381	0.033	0.031
29 ,122	0.0042	5.7	0.0701	0.0980	0.029	0.038
51 , 136	0.0018	8.9	0.0410	0.2090	0.044	0.042
18 , 171	0.0043	5.8	0.0602	0.0840	0.030	0.035
110 , 152	0.0047	11.0	0.0752	0.1813	0.031	0.036
91 , 129	0.0062	5.2	0.1426	0.1243	0.036	0.044
80 , 154	0.0009	6.8	0.0205	0.1597	0.043	0.044
45 , 164	0.0073	10.5	0.1168	0.1747	0.031	0.035
65 , 71	0.0035	9.0	0.0675	0.1798	0.035	0.037
94 , 149	0.0048	3.2	0.1123	0.0779	0.046	0.045
53 , 89	0.0008	8.3	0.0128	0.1368	0.036	0.039
35 , 142	0.0034	9.0	0.0775	0.2114	0.035	0.040
73 , 104	0.0038	5.2	0.0752	0.1065	0.036	0.041
121 , 139	0.0048	7.9	0.1085	0.1857	0.044	0.041
40 , 146	0.0020	5.5	0.0456	0.1304	0.044	0.044
78 , 172	0.0048	5.3	0.0802	0.0911	0.033	0.041

Table 6
A comparison of mass and heat transfer of $LiBr/H_2O$ solution with and without the addition of nano-particles.

Runs with similar conditions of numerical factors	With the addition of nano-particles to $LiBr/H_2O$ desiccant						R_{Gw} (%)	R_Q (%)	R_{hD} (%)	R_{hC} (%)
	$\Delta\omega_a$ (kg/kg)	ΔT_a (^{0}C)	$Gw*10^3$ (kg/s)	Q (Kw)	h_D (kg/m^{2}s)	h_C (kW/m^2^{o}C)				
1 , 46	0.0044	5.9	0.0871	0.1209	0.044	0.051	15.78	15.68	22.22	24.39
3 , 13	0.0053	4.5	0.0879	0.0769	0.043	0.047	10.41	25.00	22.86	30.55
20 , 140	0.0011	8.7	0.0176	0.1434	0.040	0.044	22.22	11.54	25.00	29.41
12 , 159	0.0047	6.1	0.0931	0.1250	0.048	0.055	17.50	19.61	23.08	25.00
38 , 161	0.0086	6.5	0.1428	0.1121	0.041	0.050	13.16	12.07	28.12	28.20
56 , 69	0.0049	7.2	0.1107	0.1692	0.041	0.053	16.67	9.09	20.59	26.19
84 , 119	0.0019	4.6	0.0317	0.0791	0.042	0.048	5.55	9.52	23.53	29.73
98 , 108	0.0023	6.4	0.0368	0.1065	0.040	0.045	15.00	10.34	25.00	32.35
64 , 160	0.0052	8.8	0.1030	0.1803	0.045	0.048	6.12	18.92	21.62	26.31
88 , 92	0.0049	9.8	0.0784	0.1631	0.041	0.040	16.67	18.07	24.24	29.03
29 ,122	0.0046	6.0	0.0768	0.1032	0.036	0.049	9.52	5.26	24.14	28.95
51 , 136	0.0019	9.7	0.0433	0.2278	0.053	0.052	5.55	8.99	20.45	23.81
18 , 171	0.0048	6.7	0.0672	0.0971	0.038	0.045	11.63	15.52	26.67	28.57
110 , 152	0.0049	12.1	0.0784	0.1994	0.037	0.045	4.25	10.00	19.35	25.00
91 , 129	0.0068	5.6	0.1564	0.1338	0.044	0.055	9.68	7.69	22.22	25.00
80 , 154	0.0010	7.9	0.0228	0.1855	0.052	0.054	11.11	16.18	20.93	22.73
45 , 164	0.0081	11.6	0.1296	0.1930	0.038	0.044	10.96	10.48	22.58	25.71
65 , 71	0.0042	10.5	0.0811	0.2098	0.043	0.047	20.00	16.67	22.86	27.02
94 , 149	0.0053	3.8	0.1240	0.0925	0.056	0.058	10.42	18.75	21.74	28.89
53 , 89	0.0010	8.9	0.0160	0.1467	0.044	0.047	25.00	7.23	22.22	20.51
35 , 142	0.0036	10.1	0.0821	0.2372	0.042	0.049	5.88	12.22	20.00	22.50
73 , 104	0.0043	6.00	0.0851	0.1229	0.044	0.051	13.16	15.38	22.22	24.39
121 , 139	0.0052	9.3	0.1175	0.2186	0.054	0.051	8.33	17.72	22.73	24.39
40 , 146	0.0023	5.9	0.0524	0.1399	0.054	0.056	15.00	7.27	22.73	27.27
78 , 172	0.0051	5.9	0.0852	0.1014	0.040	0.052	6.25	11.32	21.21	26.83

4. Conclusions

Nanofluid was prepared by adding γ-alumina nano-particles to $LiBr/H_2O$ solution as a desiccant. Air dehumidification experiments were carried out using RSM to investigate the individual and interactive effects of the six main numerical factors (air velocity, desiccant flow rate, air humidity ratio, desiccant concentration, air temperature, desiccant temperature) and one categorical factor (adding nano-particles) on outlet air humidity ratio and outlet air temperature, as responses.

CCD was used to derive reduced quadratic regression models for each response. The F values indicated that desiccant concentration had the largest effect on outlet air humidity ratio and inlet air temperature on outlet air temperature. Predictive mathematical model indicated that the optimum process conditions for the minimum outlet air humidity and temperature were at air velocity of 2.7 m/s, desiccant flow rate of 0.04 kg/s, air humidity ratio of 0.0196 kg/kg, desiccant concentration of 0.50 kg/kg, air temperature of 32.6°C, desiccant temperature of 20°C and addition of nanoparticles. The effect of nano-particles in the liquid desiccant on heat and mass transfer was investigated for the actual use of nanofluid in an air dehumidification system. It was found that average increase in mass transfer rate was 12.23 % and heat transfer rate was 13.22 %, when γ-alumina nano-

particles (0.02 wt %) were added to LiBr/H_2O solution. The mass and heat transfer coefficients were calculated using the effectiveness *NTU* model. Average increases in mass and heat transfer coefficients were 22.73 % and 26.51 %, respectively. The convective motion of nano-particles had a considerable effect on the increase in mass and heat transfer.

Nomenclature

a_w	wetted surface area of packing [m^2/m^3].
C_p	specific heat [kJ/kg ºC].
G	mass flow rate [kg/s].
G_w	mass transfer rate [kg/s].
h	enthalpy [kJ/kg].
h_C	heat transfer coefficient [kW/(m^2 ºC)].
h_D	mass transfer coefficient [kg/(m^2 s)].
Le	Lewis number, dimensionless
NTU	number of transfer unit.
Q	heat transfer rate [kW].
R	enhancement factor [%].
T	temperature [ºC].
U	velocity [m/s].
V	volume of dehumidifier [m^3].
X	mass fraction of desiccant solution [kg/kg].

Greek symbol

ω	humidity ratio [kg/kg].
λ	vaporization latent heat [kJ/kg].

Subscripts

a	air
i	inlet
o	outlet
s	desiccant solution
sat	saturation status
Ts	at solution temperature

References

[1] Fumo, N. and Goswami, D.Y., "Study of an aqueous lithium chloride desiccant system: Air dehumidification and desiccant regeneration", *Solar Energy*, **72**, 351(2002).

[2] Gandhidasan, P., "A simplified model for air dehumidification with liquid desiccant", *Solar Energy*, **76**, 409 (2004).

[3] Hassan, A.A.M. and Salah Hassan, M., "Dehumidification of air with a newly suggested liquid desiccant", *Renew. Energy.*, **33**, 1989 (2008).

[4] Li, X.W., Zhang, X.S., Wang, G. and Cao, R.G., "Research on ratio selection of a mixed liquid desiccant: Mixed LiCl–$CaCl_2$ solution", *Solar Energy*, **82**, 1161 (2008).

[5] Pahlavanzadeh, H. and Nooriasl, P., "Experimental and theoretical study of liquid desiccant dehumidification system by using the effectiveness model", *J. Therm. Sci. Eng. Appl.*, **4**, 1 (2012) .

[6] Moon, C.G., Bansal, P.K., and Jain, S., "New mass transfer performance data of a cross-flow liquid desiccant dehumidification system", *Int. J. Refrig.*, **32**, 524 (2009).

[7] Longo, G.A. and Gasparella, A., "Experimental and theoretical analysis of heat and mass transfer in a packed column dehumidifier/regenerator with liquid desiccant", *Int. J. Heat. Mass Transf.*, **48**, 5240 (2005).

[8] Omidvar Langroudi, L. and Palavanzadeh, H., "Statistical investigation of air dehumidification performance by aqueous lithium bromide

desiccant in a packed column: A thermodynamic approach", *J. Therm. Sci. Eng. Appl.*, **7**, 041013 (2015).

[9] Ren, C.Q., "Corrections to the simple effectiveness-NTU method for counterflow cooling towers and packed bed liquid desiccant–air contact systems", *Int. J. Heat. Mass Transf*., **51**, 237 (2008).

[10] Liu, X.H. and Jiang, Y., "Coupled heat and mass transfer characteristic in packed bed dehumidifier/regenerator using liquid desiccant*", Energy Convers. Manage*., 49, 1357 (2008).

[11] Luo, Y., Yang, H., Lu, L., and Qi, R., "A review of the mathematical models for predicting the heat and mass transfer process in the liquid desiccant dehumidifier", *Renew. Sustain. Energy Reviews.*, **31**, 587 (2014).

[12] Koronaki, I.P., Christodoulaki, R.I., Papaefthimiou, V.D., and Rogdakis, E.D., "Thermodynamic analysis of a counter flow adiabatic dehumidifier with different liquid desiccant materials", *Appl. Therm. Eng.*, **50**, 361 (2013).

[13] Omidvar Langroudi, L., Palavanzadeh, H. and Mousavi, S.M., "Statistical evaluation of a liquid desiccant dehumidification system using RSM and theoretical study based on the effectiveness NTU model", *J. Indust. Eng. Chem.*, **20**, 2975 (2014).

[14] Dai, Y.J., Wang, R. Z., Zhang, H. F. and Yu, J.D., "Use of liquid desiccant cooling to improve the performance of vapor compression air conditioning", *Appl. Therm. Eng*., **21**, 1185 (2001).

[15] Li, Z., Liu, X.H., Jiang, Y. and Chen, X.Y., "New type of fresh air processor with liquid desiccant total heat recovery", *Energy Build*, **37**, 587 (2005).

[16] Bassuoni, M.M., "Experimental performance study of a proposed desiccant based air conditioning system", *J. Advanced Res.*, **5**, 87 (2014).

[17] Wang, X.Q. and Mujumdar, A.S., "Heat transfer characteristics of nanofluids: A review", *Int. J. Therm. Sci.*, **46**, 1 (2007).

[18] Yang, L., Du, K., Niu, X.F., Cheng, B. and Jiang, Y.F., "Experimental study on enhancement of ammonia-water falling film absorption by adding nano-particles", Int. *J. Refrig*., **34**, 640 (2011).

[19] Zamzamian, A., Nasseri Oskouie, S., Doosthoseini, A., Joneidi, A. and Pazouki, M., "Experimental investigation of forced convective heat transfer coefficient in nanofluids of Al_2O_3/EG and CuO/EG in a double pipe and plate heat exchangers under turbulent flow", *Exp. Therm. Fluid Sci*., **35**, 495 (2011).

[20] Murshed, S.M.S., Leong, K.C., and Yang, C., "Enhanced thermal conductivity of TiO_2-water based nanofluids", *Int. J. Therm. Sci*., **44**, 367 (2005).

[21] Wen, D. and Ding, Y., "Experimental investigation into convective heat transfer of nanofluids at the entrance region under laminar flow conditions", *Int. J. Heat. Mass Transf.*, **47**, 5181 (2004).

[22] Kakac, S. and Pramuanjaroenkij, A., "Review of convective heat transfer enhancement with nanofluids", *Int. J. Heat. Mass Transf*., **52**, 3187 (2009).

[23] Fang, X., Xuan, Y. and Li, Q., "Experimental investigation on enhanced mass transfer in nanofluids", *Appl.*

Physics Letters., **95**, 203108 (2009).

[24] Feng, X. and Johnson, D.W., "Mass transfer in SiO_2 nanofluids: A case against purported nanoparticle convection effects", *Int. J. Heat. Mass Transf*., **55**, 3447 (2012).

[25] Zhu, H., Shanks, B.H. and Heindel, J.J., "Enhancing Co-water mass transfer by functionalized MCM41 nanoparticles", *Ind. Eng. Chem. Res*., **47**, 7881 (2008).

[26] Kang, Y.T., Kim, H.J., and Lee, K.I., "Heat and mass transfer enhancement of binary nanofluids for H_2O/LiBr falling film absorption process", *Int. J. Refrig*., **31**, 850 (2008).

[27] Kim, H., Jeong, J. and Tae Kang, Y., "Heat and mass transfer enhancement for falling film absorption process by SiO_2 binary nanofluids", *Int. J. Refrig*., **35**, 645 (2012).

[28] Yin, Y. and Zhang, X., "A new method for determining coupled heat and mass transfer coefficients between air and liquid desiccant", *Int. J. Heat. Mass Transf.*, **51**, 3287 (2008).

[29] Zhao-qiang, Z., Hong-ying, X., Srinivasakannan, C., Jin-hui, P. and Li-bo, Z., "Utilization of Crofton weed for preparation of activated carbon by microwave induced CO_2 activation", *Chem. Eng. Process*., **82**, 1 (2014).

[30] Jalilian Nosrati, H., Aishah Saidina Amin, N., Talebian-Kiakalaieh, A. and Noshadi, I., "Microwave assisted biodiesel production from Jatropha curcas L. seed by two-step in situ process: Optimization using response surface methodology", *Bioresource Tech*., **136**, 565 (2013).

[31] Montgomery, D.C., Design and analysis of experiments, John Wiley & Sons, New York, (2001).

[32] Khuri, A.I. and Comell, J.A., Response Surface: Design and analysis, Marcel Dekker, New York, (1987).

[33] Amani, T., Nosrati, M., Mousavi, S.M., and Kermanshahi, R.K., "Study of syntrophic anaerobic digestion of volatile fatty acids using enriched cultures at mesophilic conditions", *Int. J. Environ. Sci. and Tech*., **8**(1), 83 (2011).

[34] Zangeneh, H., Zinatizadeh, A.A.L., and Feizy, M., "A comparative study on the performance of different advanced oxidation processes ($UV/O_3/H_2O_2$) treating linear alkyl benzene (LAB) production plant's wastewater", *J. Indust. Eng. Chem*., **20**, 1453 (2014) .

Notes for Authors

Aims and Scope

The Iranian Journal of Chemical Engineering (IJChE) is a research quarterly in Chemical Engineering and related fields. The Editorial Board of the Journal tries to establish a forum for exchange of scientific findings on the core areas of the profession, as well as to cover new emerging areas and an interdisciplinary outlook of the dynamic field of Chemical Engineering. This is a peer-reviewed journal in which original contributions in the following areas appear:

- Transport Phenomena
- Thermodynamics and Phase Equilibria
- Process Design and Economics
- Separations Technology
- Mathematical Modeling and Simulation
- Process Control and Automation
- Reactions Kinetics and Catalysis
- Process Safety and Loss Prevention
- Process Technology
- Process Systems Engineering
- Biochemical Engineering
- Polymer Technology
- Reservoir Engineering
- Sustainable Development
- Energy, Combustion and Fuels
- Computer Applications and AI

State-of -the-Art and review articles, only as invited papers, will also appear in the Journal from time to time. Audience of the Journal includes industrial and academic researchers in Chemical and Process Engineering.

Preparation of Manuscripts

Contributed articles should contain new research findings which represent advances in chemical engineering research. Manuscripts are subject to peer-review by a board of referees. The average length of an article is 20 A4 pages double-spaced, including figures and tables. Contributed articles should be arranged in the following order:

Title and Authors: The title, which should be kept brief, should emphasize the principal objective. Authors' names follow the title in the next line. On a separate line, mention authors' affiliations (with addresses) where the research was done. Use an asterisk (*) to distinguish the corresponding author with a footnote containing an e-mail address of the person.

Abstract: The abstract should state the objective and conclusions of the research concisely in no more than 200 words. An additional abstract, in Persian, should accompany the manuscript. For those authors who are not familiar with Persian, the abstract is prepared by the editorial staff.

Keywords: Select a maximum of five keywords from your article that best describe the topic. These words will be used for search and retrieval, as well as indexing.

Text: Text shall start with a concise 'Introduction,' which should be free from unnecessary or non-essential details. Plain and standard English should be used for preparation of the text. It should be divided into sections with clear titles for easier reference. Authors have to either use the spell-checking facility of their word processor or proof-read the manuscript themselves before submission of the paper.

*Nomenclature*s: Symbols should be either defined in the text or entirely placed at the end of the text and immediately before the 'References' section. Symbols cited should be listed alphabetically in the order of Roman symbols, letters, subscripts and superscripts.

References: Should be listed in numerical order in the order in which they are cited in the text. Use Arabic numerals followed by a period (1., 2., etc.). The numbers must correspond to the ones used for reference within the main text (in brackets: [ ]). Give complete information, including names of all authors, titles of the article and periodicals or books, numbers of pages and volumes, and publication years. Authors should use the following style to format their references:

Journal Articles:

1. Abasaeed, A. F. and Lee, Y. Y., "Insulin hydrolysis to fructose by a novel catalyst," *Chem. Eng. Technol.*, **18** (6), 440 (1995) [**Volume** (issue number), number of the first page (year of publication)].

Books:

2. Flinn, R. A. and Trojan, P. K., Engineering materials and their applications, 3rd ed., Houghton Mifflin Co., Boston, USA, p. 144 (1986).

Proceedings:

3. Tuzunoglu, E. and Bagci, S., "Immiscible CO_2 flooding through horizontal wells for oil recovery," proceedings of *The 2nd Int. Cong. on Non-Renewable Energy Sources*, Tehran, Iran, 1, pp. 152-161 (1998).

Patents:

4. Miller, B. O., US Pat. 2542356, Dow Chemical Co., (1952).

Submission of Manuscripts

Manuscripts should be submitted online to the Journal's website: www.ijche.com

The Editorial Office Address:

The Iranian Journal of Chemical Engineering,

Unit 11, No 13 (Block 3), Maad Building, Shahid Akbari Boulevard, Azadi Ave., Tehran - Iran.

For further information on submission of papers, please contact The Editorial Office. Contact details are as follows:

Tel: +98 21 6604 2719 Fax: +98 21 6602 2196 E-mail: Secretariat@ijche.com website: www.ijche.com